Chapter 26

HRMA Focus Measurements and Raytrace Update

William Podgorski

26.1 HRMA Focus Measurements at XRCF

Two dimensional HXDS FPC pinhole scans were made on a shell-by-shell and quadrant-by-quadrant basis on three separate occasions during the Phase 1 HRMA XRCF testing period. These scans were used to calculate the best focus position of each of the four HRMA shells as well as the relative P-H tilts. We have analyzed these data and updated our raytrace model of the HRMA to include the XRCF measured focus results. We have not yet incorporated the XRCF measured intra-shell mirror tilts. In this section we describe these measurements and the subsequent analysis.

Centroids determined from a shell's quadrant images yield four pairs of coordinate values. From these, two focus estimates may be constructed:

$$\Delta_{Y,i} = 0.995\frac{\pi}{4\sqrt{2}}\frac{F}{R_i}(Y_{i,N} - Y_{i,S})$$
$$\Delta_{Z,i} = 0.995\frac{\pi}{4\sqrt{2}}\frac{F}{R_i}(Z_{i,T} - Z_{i,B})$$

where $\Delta_{Y,Z}$ are the focus error estimates; R_i is the nodal radius for the mirror pair, and F is the distance from the mirror node to the (finite conjugate) focus. (The 0.995 factor accounts for the fact that the quadrants are really only 88°.) A disagreement between these two focus error estimates may be indicative of astigmatism, either intrinsic to the optic or resulting from 1g distortions. In addition, two alignment estimators can be formed:

$$tilt_{Y,i} = 0.978\frac{\pi}{4F_i'}(Y_{i,N} + Y_{i,S} - Y_{i,T} - Y_{i,B})$$
$$tilt_{Z,i} = 0.978\frac{\pi}{4F_i'}(Z_{i,N} + Z_{i,S} - Z_{i,T} - Z_{i,B})$$

where F_i' is the distance from the body center of the H optic to the *far focus* of the H. (The 0.978 factor is a correction for 88° quadrants.)

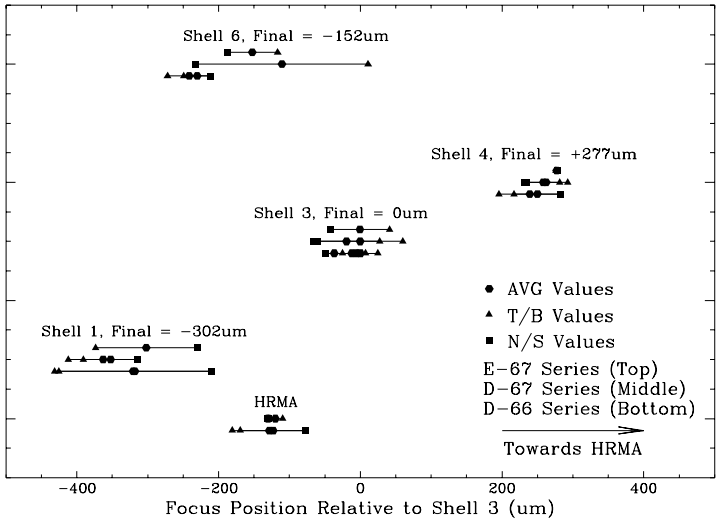

Figure 26.1: HRMA Focus Data: Focal positions are shown in μm relative to the Shell 3 focus. A positive difference represents a focus position closer to the HRMA than the Shell 3 focus (this is the XRCF sign convention and *not* that of `SAOsac`). The data are taken from three series of tests, and are shown stacked – the legend describes the stacking order. Note that there were no HRMA tests in series E-67.

The HRMA focus data from the three measurement sets performed are summarized in Figure 26.1. Five groups of data are shown, the four individual shells and the complete HRMA. For the four HRMA shells three data lines are shown, representing the initial (D-66 series), intermediate (D-67 series), and final (E-67 series) data. The focus of a shell may be calculated from either the *top* and *bottom* quadrants or the *north* and *south* quadrants. The average of these two foci was used as the shell focus position. The difference between the T/B focus and the N/S focus may be due to either astigmatism in the mirrors or to measurement error (a certain amount of separation is also induced by the 1G test environment).

The best dataset was E-67, the last one taken; more was known about the shell image qualities beforehand and more time was allocated to capture all of the flux from each quadrant of each shell, compared to the earlier data. The relative foci from these measurements are shown in Table 26.1.

Table 26.1: Best Estimate of XRCF Measured Focus of Shells, relative to Shell 3

Shell	F_N - F_3 (μm)
1	−302
3	0
4	+277
6	−152

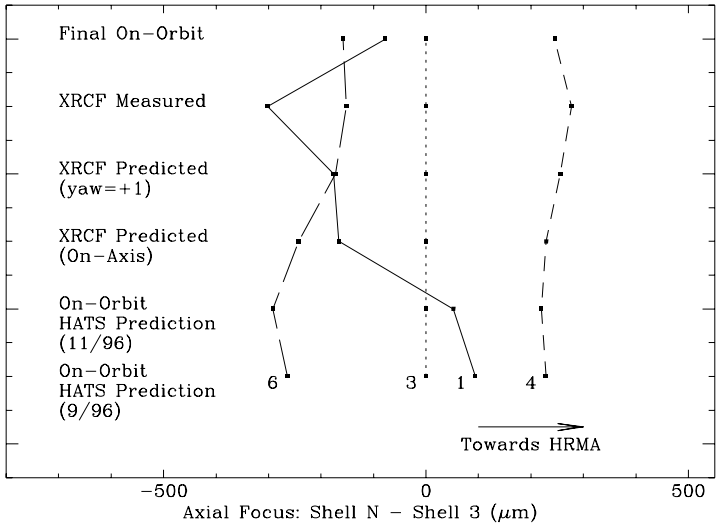

Figure 26.2: HRMA Focus History

Positive numbers represent focus positions closer to the HRMA, or shorter overall focal lengths.

In Figure 26.2 the XRCF measured focus data are compared with various focus predictions for both the on-orbit (infinite source distance, no gravity) and XRCF (finite source distance, 1G) conditions. Six different cases are shown, presented vertically with the focus values of each shell connected by lines. The bottom two cases represent the pre-calibration predictions of *on-orbit* focus from the Kodak HATS data. The bottom set of data is from the September 1996 testing, after all alignments but prior to HRMA final assembly. The next set up represents data from Kodak's November 96 HRMA Acceptance Test Procedure (ATP), after HRMA final assembly at Kodak and just prior to shipment to XRCF. Both sets of data show that the foci of the shells span about 500 μm, with the ordering of the foci as (6 – 3 – 1 – 4) in order of *decreasing* focal lengths.

The middle two cases shown in Figure 26.2 represent pre-calibration predictions of XRCF focus from the November 1996 Kodak test data, for HRMA yaw angles of both zero and one arc minute. Table 26.2 presents a comparison of predictions of the on-orbit and XRCF focal distances, relative to the P side of the HRMA CAP. The overall change in focal distance is about 195mm (longer at XRCF). However, the most interesting feature shown is that the Shell 1 focal distance increases much more (about 250 μm) than that of the other 3 shells. In Figure 26.2 this feature is shown clearly as the Shell 1 focus moves from a position between 3 and 4, for the on-orbit case, to a position further away from the HRMA, now between 6 and 3. This behavior was initially considered to be an anomaly and possibly a mistake, since raytrace studies using the *ideal* HRMA optic prescriptions and spacings did *not* give this result. However, when the as-built P1 and H1 surface prescriptions and mirror axial spacings are used this feature is seen (this result has been confirmed by Dave Zissa and Paul Glenn).

The "XRCF measured" case in Figure 26.2 shows what is considered to be the best estimate

Table 26.2: Comparison of pre-XRCF Predictions of On-orbit and XRCF HRMA foci

Shell	Focus relative to P side of CAP(mm) F_{XRCF}	$F_{\mathrm{On-Orbit}}$	ΔF	$\Delta F - \Delta F_{\mathrm{Shell3}}$
1	10274.9145004675	10079.6696878001	195.2461	0.2949
3	10274.7304206266	10079.779404296	194.9512	0.0000
4	10274.3675449462	10079.4606206727	194.9062	−0.0449
6	10274.7562744271	10079.7697370664	194.9863	0.0352

from XRCF testing of the shell-to-shell relative focus. This is from the data in Table 26.1, discussed above. We see that there is is a discrepancy of about 200 μm in the position of the Shell 1 focus at XRCF as compared with the predictions based on Kodak optical test data. At XRCF, Shell 1 had the longest focal distance, a result which was consistent over all of the testing. In discussion with L. Van Speybroeck (AXAF Telescope Scientist), we decided that the XRCF data was most likely more accurate than the Kodak optical test data, and that we should use this data as the basis for our HRMA model. The process of incorporating the XRCF data into our raytrace model is discussed below. The end result is shown as the top case in Figure 26.2. This assumption makes the predicted HRMA performance somewhat better, as the span of the foci is a bit smaller. It is now baselined in SAO's HRMA raytrace model.

26.2 Update of SAO HRMA Raytrace Model from XRCF Focus Data

In the pre-calibration SAO baseline mirror definition file, `EKCHDOS04`, the shell relative foci were set equal to those measured in the Kodak optical tests. This was done by adjusting the CAP-to-H mirror spacing so that the relative foci as determined by raytracing were equal to that measured in the optical tests. In the updated, post-calibration, SAO baseline, derived from XRCF testing, the CAP-to-mirror spacings are set to the values measured at Kodak for both P and H mirrors, and the relative foci were adjusted by making slight changes to the average cone angles of the mirrors. These cone angles were adjusted until the raytraced foci, at the XRCF finite source distance, were close to the XRCF measured relative foci. The shell 3 focus was left unchanged, and the foci of the other shells were adjusted relative to that of shell 3. The as-measured mirror data (from Kodak and HDOS) are given in Table 26.3. The data in Table 26.3 were used in the updated mirror definition file, `EKCHDOS06`.

Alteration of the cone angles was done by adding an additional "deformation" to the optics described by a Fourier-Legendre polynomial with three Legendre terms and no Fourier terms. The only non-zero term, the l_1 term, is equal to −0.001mm for the P optics and +0.001mm for the H optics (two term L-F files would have sufficed for this application). A single numerical scaling factor for these deformations was determined for each shell, and was used for both the P and H optics. The value of these multipliers was determined by trial-and-error by running tests with the full XRCF raytrace model including the `EKCHDOS06` mirror database :

Shell	Multiplier
1	0.0872
3	0.0
4	0.0150
6	0.0461

Table 26.3: As Measured Optic lengths and distances

Shell	L_P (mm)	L_H (mm)	CAP (mm)	P-CAP (in)	H-CAP (in)	ZC_P (mm)	ZC_H (mm)
1	842.2150	842.1920	49.911	0.2153	0.3940	-426.5761	481.0146
3	842.2080	842.1970	49.911	0.6144	0.3905	-436.7098	480.9282
4	842.2080	842.2250	49.911	0.7580	0.3860	-440.3572	480.8279
6	842.2090	842.2000	49.911	0.9440	0.3230	-445.0821	479.2152

L_P Length of P Mirror
L_H Length of H Mirror
CAP Thickness of CAP
P-CAP Distance from P side of CAP to P mirror
H-CAP Distance from H side of CAP to H mirror
ZC_P Z co-ordinate of center of P mirror in SAO raytrace co-ordinates
ZC_H Z co-ordinate of center of H mirror in SAO raytrace co-ordinates

Table 26.4: Final Mirror Focal Positions at XRCF and on orbit

	XRCF			On Orbit	
	Raytrace		Meas.	Raytrace	
Shell	F_N (mm)	-(F_N - F_3) (μm)	F_N - F_3 (μm)	F_N (mm)	-(F_N - F_3) (μm)
1	10275.0342	-305	-302	10079.8359	-77
3	10274.7295	0	0	10079.7588	0
4	10274.4551	274	277	10079.5137	245
6	10274.8730	-144	-152	10079.9170	-158

The resultant deformations are summed with the other mirror distortions to create the final mirror maps.

In Table 26.4, raytrace results using these offset files plus the new `EKCHDOS06` mirror database are given for both the XRCF and on-orbit cases, plus the measured XRCF relative foci (repeated for convenience from Table 26.1. The raytraced F_N are measured relative to the P side of the CAP in the raytrace (`SAOsac`) coordinate system. The foci relative to Shell 3 are presented in the XRCF coordinate system (recall from Figure B.1 that the `SAOsac` Z optical axis coordinate is flipped with respect to the XRCF X coordinate). A positive relative focus again indicates a focus value closer to the HRMA. The results from the on-orbit raytrace (the last column in Table 26.4) are also plotted as "Final On-Orbit" in Figure 26.2.

Test data are given in Tables 26.5 through 26.7.

Table 26.5: Test Data for HRMA Focus Tests: D-66 Series

Date	TRW Test ID	Shell	PrimeX [μm]	δF_y [μm]	δF_z [μm]	Yaw [$'$]	Pitch [$'$]
01/02/97	D-IXF-P2-66.001	3	−32566	180.8	178.7	0	0
01/02/97	D-IXF-P2-66.002						
01/02/97	D-IXF-P2-66.003						
01/02/97	D-IXF-P2-66.004						
01/02/97	D-IXF-P2-66.005	3	−32566	180.8	166.8	0	0
01/02/97	D-IXF-P2-66.002						
01/02/97	D-IXF-P2-66.003						
01/02/97	D-IXF-P2-66.004						
01/02/97	D-IXF-P2-66.026	3	−32804	−15.0	−39.1	0	0
01/02/97	D-IXF-P2-66.027						
01/02/97	D-IXF-P2-66.028						
01/02/97	D-IXF-P2-66.029						
01/02/97	D-IXF-P2-66.030	3	−32804	−15.0	−88.8	0	0
01/02/97	D-IXF-P2-66.027						
01/02/97	D-IXF-P2-66.028						
01/02/97	D-IXF-P2-66.029						
01/02/97	D-IXF-P2-66.006	4	−32563	−106.0	−18.7	0	0
01/02/97	D-IXF-P2-66.007						
01/03/97	D-IXF-P2-66.008						
01/03/97	D-IXF-P2-66.009						
01/03/97	D-IXF-P2-66.010	4	−32563	−106.0	−40.0	0	0
01/03/97	D-IXF-P2-66.007						
01/03/97	D-IXF-P2-66.008						
01/03/97	D-IXF-P2-66.009						
01/03/97	D-IXF-P2-66.011	6	−33060	−108.9	−47.9	0	0
01/03/97	D-IXF-P2-66.012						
01/03/97	D-IXF-P2-66.013						
01/03/97	D-IXF-P2-66.014						
01/03/97	D-IXF-P2-66.015	6	−33060	−108.9	−70.7	0	0
01/03/97	D-IXF-P2-66.012						
01/03/97	D-IXF-P2-66.013						
01/03/97	D-IXF-P2-66.014						
01/03/97	D-IXF-P2-66.016	1	−32962	−11.5	209.2	0	0
01/03/97	D-IXF-P2-66.017						
01/03/97	D-IXF-P2-66.018						
01/03/97	D-IXF-P2-66.019						
01/03/97	D-IXF-P2-66.020	1	−32962	−11.5	203.2	0	0
01/03/97	D-IXF-P2-66.017						
01/03/97	D-IXF-P2-66.018						
01/03/97	D-IXF-P2-66.019						

Table 26.5: Test Data for HRMA Focus Tests: D-66 Series, continued

Date	TRW Test ID	Shell	PrimeX [μm]	δF_y [μm]	δF_z [μm]	Yaw [′]	Pitch [′]
01/03/97	D-IXF-P2-66.021	1346	−32866	−49.4	54.7	0	0
01/03/97	D-IXF-P2-66.022						
01/03/97	D-IXF-P2-66.023						
01/03/97	D-IXF-P2-66.024						
01/03/97	D-IXF-P2-66.025	1346	−32866	−49.4	43.2	0	0
01/03/97	D-IXF-P2-66.022						
01/03/97	D-IXF-P2-66.023						
01/03/97	D-IXF-P2-66.024						

Table 26.6: Test Data for HRMA Focus Tests: D-67 Series

Date	TRW Test ID	Shell	PrimeX [μm]	δF_y [μm]	δF_z [μm]	Yaw [′]	Pitch [′]
01/05/97	D-IXF-P2-67.001	3	−32782	41.5	−52.6	−1	0
01/05/97	D-IXF-P2-67.002						
01/05/97	D-IXF-P2-67.003						
01/05/97	D-IXF-P2-67.004						
01/05/97	D-IXF-P2-67.005	3	−32776	41.5	−79.0	−1	0
01/05/97	D-IXF-P2-67.002						
01/05/97	D-IXF-P2-67.003						
01/05/97	D-IXF-P2-67.004						
01/05/97	D-IXF-P2-67.006	4	−32499	22.9	−23.1	−1	0
01/05/97	D-IXF-P2-67.007						
01/05/97	D-IXF-P2-67.008						
01/05/97	D-IXF-P2-67.009						
01/05/97	D-IXF-P2-67.010	4	−32502	22.9	−37.9	−1	0
01/05/97	D-IXF-P2-67.007						
01/05/97	D-IXF-P2-67.008						
01/05/97	D-IXF-P2-67.009						
01/05/97	D-IXF-P2-67.011	6	−32984	5.3	−238.1	−1	0
01/05/97	D-IXF-P2-67.012						
01/06/97	D-IXF-P2-67.013						
01/06/97	D-IXF-P2-67.014						
01/06/97	D-IXF-P2-67.015	6	−32984	5.3	−238.1	−1	0
01/06/97	D-IXF-P2-67.012						
01/06/97	D-IXF-P2-67.013						
01/06/97	D-IXF-P2-67.014						
01/06/97	D-IXF-P2-67.016	1	−33058	12.9	111.1	−1	0
01/06/97	D-IXF-P2-67.017						
01/06/97	D-IXF-P2-67.018						
01/06/97	D-IXF-P2-67.019						
01/06/97	D-IXF-P2-67.020	1	−33058	12.9	89.9	−1	0
01/06/97	D-IXF-P2-67.017						
01/06/97	D-IXF-P2-67.018						
01/06/97	D-IXF-P2-67.019						
01/06/97	D-IXF-P2-67.021	1346	−32861	26.3	26.0	−1	0
01/06/97	D-IXF-P2-67.022						
01/06/97	D-IXF-P2-67.023						
01/06/97	D-IXF-P2-67.024						
01/06/97	D-IXF-P2-67.025	1346	−32861	26.0	5.6	−1	0
01/06/97	D-IXF-P2-67.022						
01/06/97	D-IXF-P2-67.023						
01/06/97	D-IXF-P2-67.024						

Table 26.7: Test Data for HRMA Focus Tests: E-67 (Final) Series

Date	TRW Test ID	Shell	PrimeX [μm]	δF_y [μm]	δF_z [μm]	Yaw [′]	Pitch [′]
02/07/97	E-IXF-P2-67.001	3	−32562	−282.03	−365.2	0	0
02/07/97	E-IXF-P2-67.002						
02/07/97	E-IXF-P2-67.003						
02/07/97	E-IXF-P2-67.004						
02/07/97	E-IXF-P2-67.006	4	−31970	−9.64	−8.2	0	0
02/07/97	E-IXF-P2-67.007						
02/07/97	E-IXF-P2-67.008						
02/07/97	E-IXF-P2-67.009						
02/07/97	E-IXF-P2-67.011	6	−32341	85.09	13.6	0	0
02/07/97	E-IXF-P2-67.012						
02/07/97	E-IXF-P2-67.013						
02/07/97	E-IXF-P2-67.014						
02/07/97	E-IXF-P2-67.016	1	−32589	−120.6	22.6	0	0
02/07/97	E-IXF-P2-67.017						
02/07/97	E-IXF-P2-67.018						
02/07/97	E-IXF-P2-67.019						

26.3 Updated deformation and sum files

In `SAOsac` terminology Legendre-Fourier DFR "offset" files were created to describe the deformation to the optics which provides the required change in optic cone angle:

pN`_off.DFR` (where $N = 1, 3, 4, 6$):

```
P  Deformation                                              3    0
   0.00000E+00   -1.00000E-03    0.00000E+00
```

hN`_off.DFR` (where $N = 1, 3, 4, 6$):

```
H  Deformation                                              3    0
   0.00000E+00    1.00000E-03    0.00000E+00
```

So-called "sum" files direct the summation of the various distortions and their magnitudes (i.e. the scaling factor mentioned above). The Shell 1 files look like this:

`p1_xrcf_sum_off.files` :

```
p1_xrcf_sum_off.SPL 422 288
/proj/axaf/Syseng/models/hrma-xrcf/xrcf_2wks/p1_xrcf_sum.SPL 1.000 0.000
p1_off.DFR 0.0872 0.000
```

`h1_xrcf_sum_off.files` :

```
h1_xrcf_sum_off.SPL 422 288
/proj/axaf/Syseng/models/hrma-xrcf/xrcf_2wks/h1_xrcf_sum.SPL 1.000 0.000
h1_off.DFR 0.0872 0.000
```

The "sum" files have names of the form *xn*`_xrcf_sum_off.SPL` where x = {p, h} and n = {1, 3, 4, 6}.

All of these files are located in

`/proj/axaf/Syseng/models/hrma-xrcf/xrcf_2wks_offset/`

on the CfA Central Engineering and High Energy Astrophysics LANs.